Received: 27 July 2019 | Accepted: 3 January 2020

DOI: 10.1002/jor.24607

RESEARCH ARTICLE

Journal of Orthopaedic Research®

Oxytocin-loaded sustained-release hydrogel graft provides accelerated bone formation: An experimental rat study

Ayse Sumeyye Akay[1] | Volkan Arısan[1] | Erdal Cevher[2] | Melike Sessevmez[2] | Betul Cam[3]

[1]Department of Oral Implantology, Faculty of Dentistry, Istanbul University, Istanbul, Çapa, Turkey

[2]Department of Pharmaceutical Technology, Faculty of Pharmacy, Istanbul University, Istanbul, Turkey

[3]Department of Physiology, Uludag University School of Medicine, Bursa, Turkey

Correspondence
Volkan Arısan, Department of Oral Implantology, Faculty of Dentistry, Istanbul University, Capa, 34093 Istanbul, Turkey.
Email: varisan@istanbul.edu.tr

Present address
Ayse Sumeyye Akay, Department of Oral & Maxillofacial Surgery, Faculty of Dentistry, Istanbul Medeniyet University, Istanbul, Turkey. Betul Cam, Department of Emergency Medicine, Education and Training Hospital of Bagcilar, Istanbul, Turkey.

Funding information
Türkiye Bilimsel ve Teknolojik Arastirma Kurumu, Grant/Award Number: 2211; Bilimsel Arastirma Projeleri Birimi, Istanbul Üniversitesi, Grant/Award Number: 50527

Abstract

Restoration of the lost bone volume is one of the most deliberate issues in dentistry. Sustained-release microspherical oxytocin hormone in a poloxamer hydrogel scaffold combined with a mixture of β-tricalcium phosphate and hydroxyapatite (CP) may serve as a suitable bone graft. The aim of this study was to design and test a novel thermosensitive hydrogel graft incorporating oxytocin-loaded poly(D, L-lactide-co-glycolide) (PLGA) sustained-release microspheres and CP. Thermosensitive poloxamer hydrogel containing CP (HCP graft) was prepared as a base and combined with hollow microspheres (HCPM) and oxytocin-loaded microspheres (HCPOM). Eighty Wistar rats were used for testing the grafts and a control group in 8-mm-diameter critical-sized calvarial defects (CSD); (n = 20). Bone healing at the 4th and 8th weeks was evaluated by histological, histomorphometric, and radiological (micro-computed tomography [μCT]) analyses. The results were analyzed by two-way analysis of variance ($P < .05$). Oxytocin-loaded PLGA microspheres prepared by the solvent displacement method yielded a high encapsulation efficiency of 89.5% and a slow drug release. Incorporation of the microspheres into the hydrogel graft slowed the release rate down and the release completed within 32 days. HCPOM revealed the highest new bone formation (26.45% ± 6.65% and 30.76% ± 4.37% at the 4th and 8th weeks, respectively; $P < .0001$) while HCPM and HCP groups revealed a bone formation of around 10% ($P > .05$). μCT findings of HCPOM group showed the highest mean bone mineral density values (42.21 ± 5.14 and 46.94 ± 3.30 g/cm^3 for the 4th and 8th weeks, respectively; $P < .0027$). The proposed oxytocin-loaded sustained-release PLGA microspheres containing thermosensitive hydrogel graft (HCPOM) provide an accelerated bone regeneration in the rat calvaria.

KEYWORDS

bone regeneration, oxytocin, sustained-release, poly(D, L-lactide-co-glycolide) microsphere, hydrogel

1 | INTRODUCTION

Restoration of the lost bone volume is one of the central concerns in oral and maxillofacial interventions. A variety of biological products and synthetic materials have been utilized as bone substitutes which all have specific advantages and disadvantages.[1,2] Autogenous bone grafts have osteoinductive properties, but their retrieval is challenging and costly while alloplasts are affordable but lack osteoinductive features and serve as a space-maintainer only.[3,4] Calcium phosphates, despite their high biocompatibility and beneficial effect on cell differentiation for bone formation,[1,2] have failed to achieve complete biodegradation and bone replacement without the use of an inductive agent[5,6] or combining a biodegradable compound.[7] However, the outcomes of the attempts to overcome such drawbacks were mostly controversial, probably due to the lack of specific induction of bone regeneration via intramembranous mechanisms.[8]

Oxytocin is a primitive neurohypophysial anabolic hormone enrolled in lactation of mammals that also provides local autocrine and paracrine effects for bone metabolism besides the systemic endocrine pathway.[9] The systemic application of this hormone enhances bone formation by positive modulation of osteoblast differentiation, osteoclast functions, and up-regulation of bone morphogenic protein-2 (BMP-2).[10,11] Although oxytocin was studied in many different medical applications, its effect on local bone regeneration has not been investigated probably due to its short half-life and the poor stability against the hydrolytic enzymes.[12] Without an appropriate carrier and encapsulating method, the influence of this hormone is momentary, and the physicochemical stability could not be maintained during the bone healing period. In this regard, poly(D, L-lactide-co-glycolide) PLGA copolymers have been utilized as the carrier of different biomaterials to formulate sustained-release systems, especially for the peptides and proteins due to their long clinical experience, desirable degradation characteristics, biocompatibility, and relevant FDA approval.[13]

The manipulation of the grafting materials are also critical, and injectable forms were favored due to their clinical feasibility.[3] Hydrogels have been studied for such purposes since they serve as a biomimetic network of hydrophilic polymer chains that allow infiltration of cells and diffusion of molecules throughout the structure in an injectable carrier form, especially for peptide and protein drugs[14,15]—such as oxytocin. Amongst the so-called "smart thermogelling injectable hydrogels", the poloxamers have been under attention due to the sol-to-gel transition upon heating towards the body temperature. Their reconfigurability enables them to be used as a biodegradable transfer medium catering sustained-release of oxytocin in the desired area.[16] These biocompatible and biodegradable polymeric materials are opportune candidates for the design of a new biomaterial that would satisfy the biological requirements and endorse bone regeneration.

In this study, a novel thermosensitive hydrogel bone graft combined with oxytocin-loaded PLGA microspheres and a mixture of β-tricalcium phosphate and hydroxyapatite powder (CP) was designed and tested in 8-mm-diameter critical-sized rat calvarial defects, in vivo.

2 | MATERIALS AND METHODS

2.1 | Materials

PLGA with lactic to glycolic acid ratio of 50:50 (Resomer RG 502H; Sigma-Aldrich, St Louis), Oxytocin in crystalized particulate form (527 IU/mg; DEVA, Istanbul, Turkey), Acetone (Merck KGaA, Darmstadt, Germany), Poloxamer P407 (Lutrol F127; BASF, Ludwigshafen, Germany), hydroxyapatite (HA, hydroxyapatite powder; Sigma-Aldrich) β-tricalcium phosphate (β-TCP; Sigma-Aldrich), dimethyl sulfoxide (DMS; Merck KGaA), and dichloromethane (DCM; Merck KGaA). All the other chemicals are in analytical grade.

2.2 | Preparation of the oxytocin-loaded PLGA microspheres

Microspheres (OM) were prepared with the solvent displacement method. Briefly, 100 mg PLGA was dissolved in 15 mL acetone, and 10 mg oxytocin was dispersed in the PLGA solution. The mixture was then added dropwise to the 15 mL of distilled water under magnetically stirring at 300 rpm. After 5 minutes of stirring, the organic solvent was evaporated (Rotary Evaporator RV 10 control; IKA, Wilmington) at the room temperature. The resultant microspheres were separated by centrifugation (Allegra X-30; Beckman, Indianapolis) at 15 000 rpm for 1 hour at 4°C, washed three times with purified water and lyophilized (VirTis AdVantage Plus; SP Scientific, Warminster) at −50°C for 72 hours. Microspheres were weighed. The production yield was determined gravimetrically using the following equation. Each formulation was carried out in triplicate. Blank microspheres (M) were prepared as positive controls.

$$\text{Production yield}(\%) = \frac{\text{Weigh of the microspheres}}{\text{Total solids}(\text{PLGA} + \text{oxytocin})}.$$

2.2.1 | Loading capacity and encapsulation efficiency of the microspheres

Ten miligram microspheres were accurately weighed and dissolved in 1 mL of DMS and DCM mixture at a ratio of 1:4. Ten milliliter distilled water was added, and the mixture was vortexed for 10 minutes, then shaken for 1 hour. The aqueous phase was centrifugated at 10 000 rpm and analyzed for oxytocin content using UV spectrophotometry (UV-1601, UV-Visible Spectrophotometer; Shimadzu, Kyoto, Japan) at 276 nm. Loading capacity[16] and encapsulation efficiency (EE) was calculated using the following equation. All analyses were carried out in triplicate.

$$\text{LC}(\%) = \frac{M_{\text{act}}}{\text{Weigh of the microspheres}},$$

$$\text{EE}(\%) = \frac{M_{\text{act}}}{M_{\text{the}}} \times 100,$$

where M_{act} is the actual oxytocin content in the weighed quantity of microspheres, M_{the} is the theoretical amount of oxytocin in microspheres calculated from the quantity added in the process.

2.2.2 | Characterization of the microspheres

The particle size and size distribution (polydispersity index [PDI]) of microspheres were determined by photon correlation spectroscopy (Nano-ZS; Malvern Instruments, Malvern, UK) at 25°C ($n = 3$). The zeta potential of microspheres was determined by using an electrophoretic light-scattering technique (Zetasizer Nano-ZS; Malvern Instruments) ($n = 6$). The morphology of microspheres was investigated using Scanning electron microscopy (SEM; FEI QuantaTM FEG 450; Thermo Fisher Scientific, MA) at 25 kV.

2.3 | Gelation temperature of poloxamer solutions

To determine the optimal poloxamer concentration in the experimental bone grafts, poloxamer solutions with a concentration between 18% and 23% were prepared by dissolving Poloxamer P407 in 100 mL distilled water at 5°C by stirring on a magnetic stirrer at 400 rpm. The sol-gel transition of poloxamer solutions was measured using viscometer (Brookfield RVDV-II+; Brookfield Laboratories, Stoughton) depending on the increase in temperature from 18°C up to 37°C.

2.4 | Preparation of hydrogel grafts

The base graft compound (HCP) was prepared by mixing the poloxamer solution (23%, w/v) with 150 mg of the CP mixture which is composed of HA/β-TCP (60:40, w/w). Then, 250 μg of oxytocin (O) or 2.8 mg of empty PLGA microspheres (M) or oxytocin-loaded PLGA microspheres (OM) equivalent to 250 μg of oxytocin (2.8 mg) was incorporated into the HCP to fabricate the HCPO, HCPM, and HCPOM grafts, respectively (Figure 1). All grafts were placed in 1 mL sterile syringes and were kept in the cold (2-8°C) until the administration.

2.5 | In vitro release

Oxytocin-loaded PLGA microspheres equivalent to 10 mg oxytocin, hydrogel graft containing 10 mg oxytocin and hydrogel graft containing oxytocin-loaded PLGA microspheres equivalent to 10 mg of oxytocin were placed in separate Eppendorf tubes, and 1.5 mL pH 7.4 phosphate buffer saline (PBS) was added to each tube. The tubes were shaken at 150 rpm in an orbital shaker (Forma orbital shaker; Thermo Fisher Scientific, MA) thermostated at 37 °C ± 1°C. At the scheduled time intervals (from 2 hours to 32 days), the tubes were centrifuged at 5000 rpm for 5 minutes; 1.4 mL samples were withdrawn and replaced with fresh medium. The samples were filtered through 0.45 μm membrane filter (Millipore; Merck, Philadelphia) and the quantification of drug content was performed by UV spectrophotometry. All analyses were carried out in triplicate.

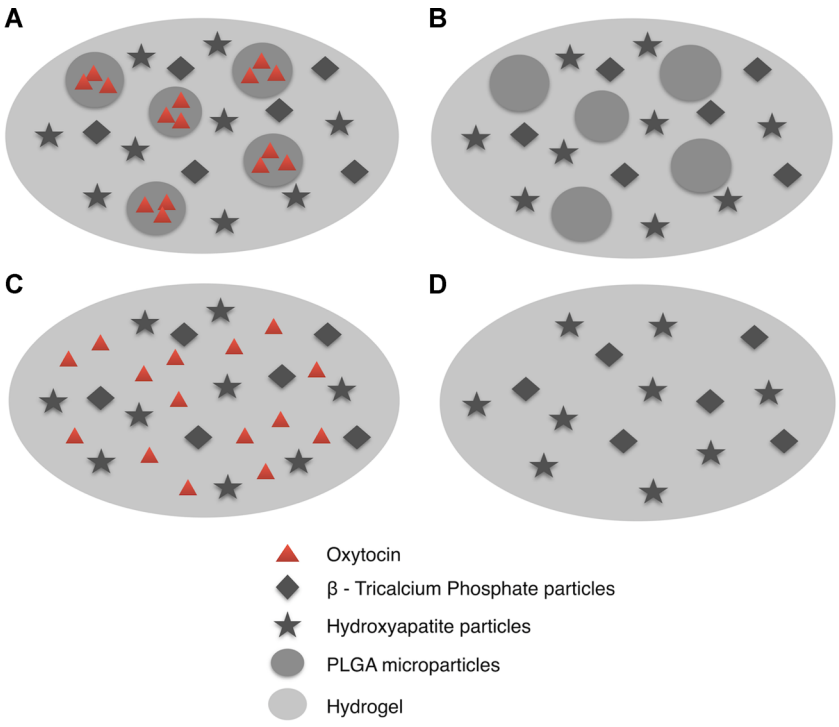

FIGURE 1 A, Oxytocin-loaded PLGA microspheres and CP containing hydrogel graft (HCPOM). B, Blank PLGA microspheres and CP containing hydrogel graft (HCPM). C, Free oxytocin and CP containing hydrogel graft (HCPO). D, CP containing hydrogel graft (HCP). PLGA, poly(D, L-lactide-co-glycolide) [Color figure can be viewed at wileyonlinelibrary.com]

2.6 | Animal experiment

The study was approved by the Local Ethical Committee for Animal Experiments of Uludag University (UUHADYEK; protocol 2015-04/03) under the guidelines of institutional laboratory animal care and national laws on animal use.

Eighty adult (16-week-old) male Wistar rats (250 ± 30 g) were acquired from the Uludag University Research Center of Laboratory Animals. The animals were maintained at 21 to 24°C and 40% to 60% relative humidity on a 12/12-h light/dark cycle and were housed in plastic cages having free access to water and standard laboratory rodent food. The animals were divided into eight groups ($n = 10$) according to the proposed time intervals of each three graft formulations described above (HCP, HCPM, and HCPOM) and one empty control group.

2.6.1 | Surgical procedure

Intraperitoneal injection of ketamine (100 mg/kg, Ketalar Flakon; Pfizer, Istanbul, Turkey) and xylazine (10 mg/kg, Rompun Flakon; Bayer, Istanbul, Turkey) was administered for general anesthesia. Hair of the head was shaved and cleaned with povidone iodine. A 2.5 cm anteroposterior incision from the nasofrontal region to the external occipital protuberance was made and the skull was exposed. Bregma was referred to as the mid-frontal point for the standardization of the defects. Using an 8-mm-diameter surgical trephine bur attached to a surgical hand-piece, a critical-sized 8-mm-diameter full-thickness calvarial defect[17] was created under sterile saline irrigation. Care was given to prevent underlying Dura mater (Figure 2). Grafts were applied to the defects and shaped to the geometry of calvarial bone. Twenty defects were left empty to serve as the control group. The periosteum and skin were closed with sutures (Vicryl; Ethicon, NJ). Rats were placed in single cages. A total of 3 mg/kg gentamycin (20 mg/mL, Gentamed; KocakFarma, Istanbul, Turkey) and 1 mg/kg metamizole sodium (Novalgin; Sanofi Aventis, Istanbul, Turkey) were subcutaneously administered for 3 days. The sutures were removed after 10 days. Then the animals were transferred to double cages.

2.6.2 | Fluorochrome labeling

To determine the onset time and location of osteogenesis, in vivo fluorochrome labeling was performed as proposed before.[18,19] A total of 30 mg/kg Alizarin (Alizarin Red-S; Sigma-Aldrich) 10 days after the surgery, and 20 mg/kg calcein green (calcein; Sigma-Aldrich) were administered 15 days before the sacrification via penile vein intravenously.[20,21]

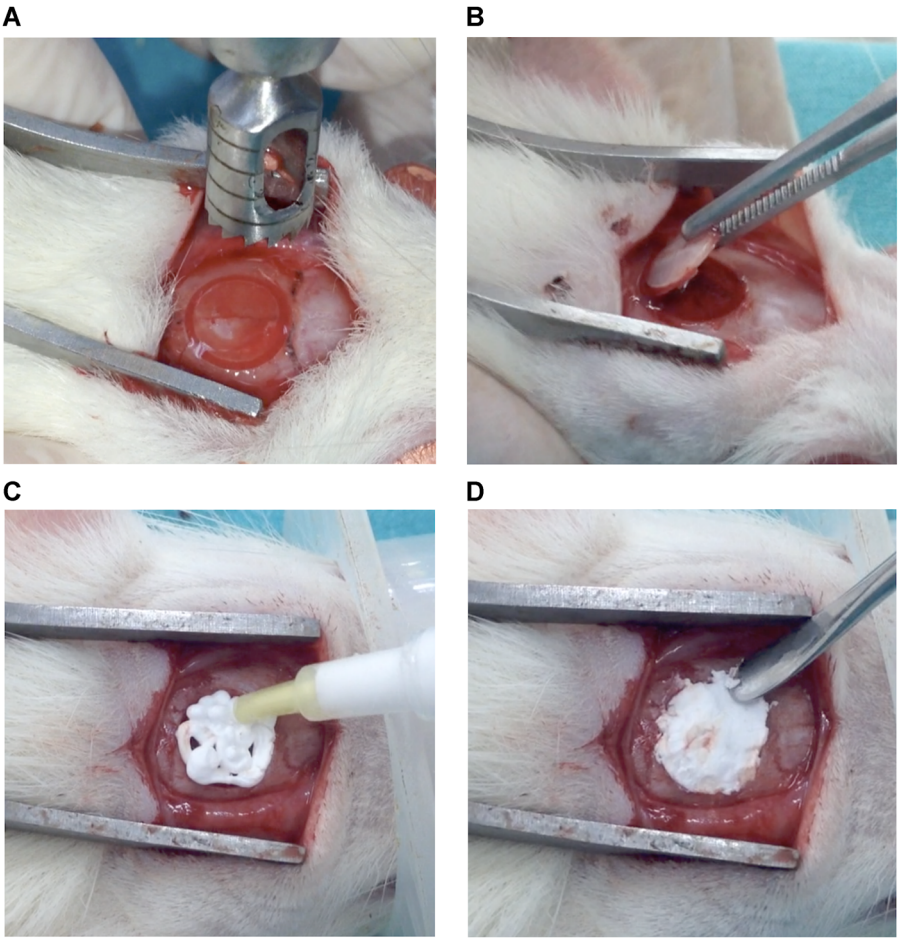

FIGURE 2 A, B, Preparation of the 8-mm-diameter critical-sized defect on the rat calvaria. C, D, Injection and application of the hydrogel graft [Color figure can be viewed at wileyonlinelibrary.com]

2.6.3 | Retrieval of the samples

At the end of the 4th and 8th weeks, the rats were euthanized by intraperitoneal injection of sodium pentothal. Calvarial bones, including parietal and frontal bones, were harvested en-bloc, and immediately immersed in 10% phosphate-buffered formalin (pH = 7.4) for fixation.

2.7 | Micro-computed tomography analysis

New bone formation was quantified on all samples by an X-ray micro-computed tomography (μCT); scanning was performed by a 71.76 μm pixel camera-connected device (SHT MR285MC; Bruker, MA) with an exposure of 6000 ms, in CC gantry position. Image data were acquired, reconstructed in "TIFF" format (SkyScan NRecon 1.6.10.2; Bruker) with 61.01 μm "Image Pixel Size", and were converted to axial projection of the skull (DataViewer; Bruker SkyScan-MicroCT, MA). A circular region of interest (ROI) consisting of the defect area was determined for quantitative analysis. Bone volume (BV; mm^3) and bone mineral density (BMD; g/cm^3) were analyzed (CT-Analyser 1.15.4.0; Bruker).

2.8 | Histological analysis

Bone sections were prepared according to the non-decalcified protocol[22,23] using the EXAKT grinding system (Exakt Apparatbau; Norderstedt, Germany). One standardized section in the vertical-coronal plane enclosing the full diameter of the defect was prepared for all samples in 40 μm thickness, stained with Goldner's Masson Trichrome[24] except one-single section in each group for fluorescence imaging. Sections were examined by relevant digital camera connected light microscope (Olympus ε-330 and Olympus CX41; Tokyo, Japan), and fluorescence microscope attached digital camera (Olympus BX51 and Olympus U-CMAD3; Tokyo, Japan).

2.9 | Histomorphometric analysis

Digital images (4000 × 3000 pixels, 300 pixels/inch) were taken by a digital camera connected stereomicroscope (Nikon CoolPix P5100 and Nikon SMZ1000, Tokyo, Japan), and were analyzed with a computer image analysis software (Fiji GNU; SciJava, Osaka, Japan). A circular ROI was defined (differs in a range of 50-70 mm^2 according to each subject). New bone formation (NB) and residual graft (RG) were measured in pixel units and were expressed as percentage (Figure 3).

2.10 | Statistical analysis

An estimated minimum number of 9.55 rats per group with reference to similar studies[25,26] was calculated to detect a 30% difference of new bone formation between the designated groups and time intervals at the level of $\alpha = .05$ and with a statistical power of 80% (nQuery Advisor; Statistical Solutions, Saugus). Mean and standard deviation (SD), range and 95% confidence interval (CI) were calculated. The normality of the distribution was analyzed using D'agostino Pearson Omnibus Test. Two-way analysis of variance (ANOVA) was used for the change of the group variables according to the different time intervals. Tukey's post-hoc test was used for pairwise comparisons (GraphPad Prism 7.1; GraphPad Software, San Diego). A P value of <.05 was considered statistically significant.

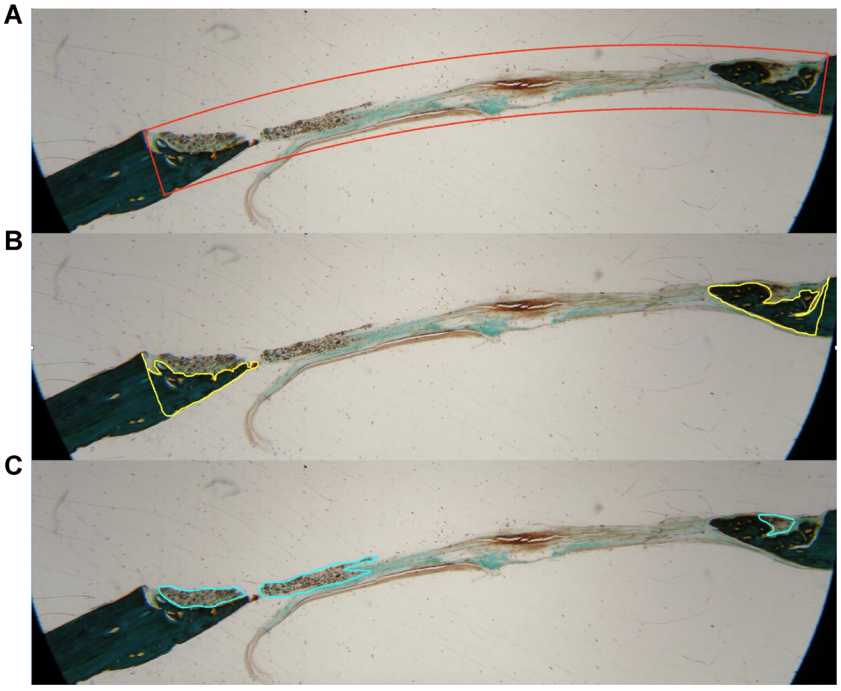

FIGURE 3 Measurement areas in the histomorphometric analysis. A, Initial defect area is marked by red color. B, The new bone area is marked by yellow color. C, Remnants of the hydrogel graft are marked by turquoise color. Section belongs to the HCPOM group. Goldner's Masson Trichrome staining, original magnification x10 [Color figure can be viewed at wileyonlinelibrary.com]

ARRIVE guidelines were followed in the execution of the animal experiments and preparation of the manuscript.

3 | RESULTS

3.1 | Preparation and characterization of microspheres

Oxytocin-loaded microspheres prepared by the solvent displacement method. Total, 13.18% of the loading capacity, 61.75% of the production yield and 89.53% of the EE were obtained with the mentioned particle preparation method (Table 1).

The particle size of the microspheres was 1.64 ± 0.18 μm, and their polydispersity index was 0.252. Particle morphology was evaluated with scanning electron microscopy, and oxytocin-loaded microspheres presented a well-designed spherical morphology with a smooth surface (Figure 4).

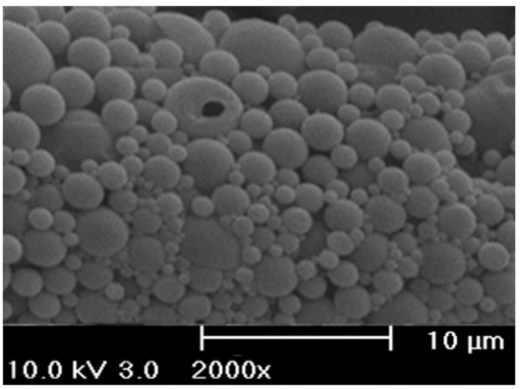

FIGURE 4 Scanning electron microphotograph of oxytocin-loaded PLGA microspheres, original magnification ×2000. PLGA, poly (D, L-lactide-co-glycolide)

3.2 | Optimization of hydrogel formulations

Different concentrations of poloxamer in water (between 18% and 23%) at 10°C were prepared and their sol-gel transitions were measured using viscometer depending on increase in temperature from 18°C up to 27°C to determine the best concentration which is easily applicable at lower temperatures and is retained for a long time in the cavity around body temperature. The viscosity of the hydrogels was affected by the concentration of the polymer as well as by the ambient temperature. While the viscosity (18-23%) did not significantly change up to 20°C; over this temperature value, the viscosity began to increase rapidly up to the temperature of 27°C (Figure 5). As a result of that, hydrogel at the concentration of 23% was chosen as an implantable carrier system for oxytocin and oxytocin-loaded microspheres.

Suitability of hydrogels as a graft material was also observed in in vivo conditions. The manipulation of the hydrogel grafts was easy in situ, and the hydrogels were set within 5 minutes, and were not affected by local bleeding, which was described as the "wash-out" effect regarding the other injectable graft materials.[27,28]

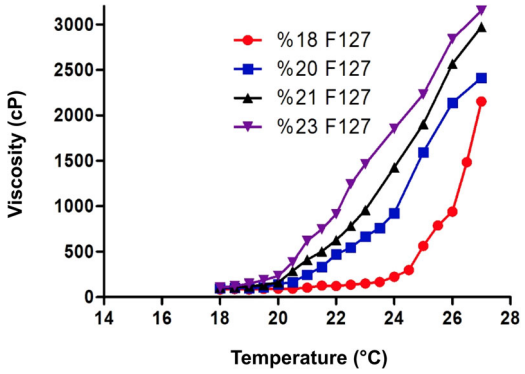

FIGURE 5 Temperature-dependent viscosity changes of poloxamer hydrogels prepared with different polymer concentration from 18% to 23% [Color figure can be viewed at wileyonlinelibrary.com]

3.3 | In vitro release

The drug release from microspheres and hydrogel formulations were measured by the dialysis method in pH 7.4 phosphate buffer at 37°C (Figure 6). The free oxytocin containing hydrogel graft (HCPO) showed the fastest release rate, and oxytocin was released entirely within three days. A reduction in drug release was observed when oxytocin was incorporated into the microspheres. Around 51% and 42% of oxytocin from oxytocin-loaded microspheres (OM) and oxytocin-loaded microspheres containing hydrogel graft (HCPOM), respectively, were released in the 1st week. Then the release slowed down and completed within 29 days from OM and 32 days from HCPOM. As seen in Figure 5, microspheres and poloxamer/microsphere combinations significantly extended the release of oxytocin.

3.4 | Micro-CT

A prominent growth of new bone was observable in the HCPOM group, whereas the healing pattern was resembling the control in the

TABLE 1 Particle size and size distribution (polydispersity index [PDI]), zeta potential, production yield, encapsulation efficiency, and loading capacity of oxytocin-loaded PLGA microspheres (n = 3)

Particle size ± SD, μm	Polydispersity	Zeta potential ± SD, mV	Production yield ± SD, %	EE ± SD, %	Loading capacity ± SD, %
1.64 ± 0.18	0.252	−17.4 ± 0.7	61.75 ± 5.8	89.53 ± 6.2	13.18 ± 1.2

Abbreviations: EE, encapsulation efficiency; SD, standard deviation.

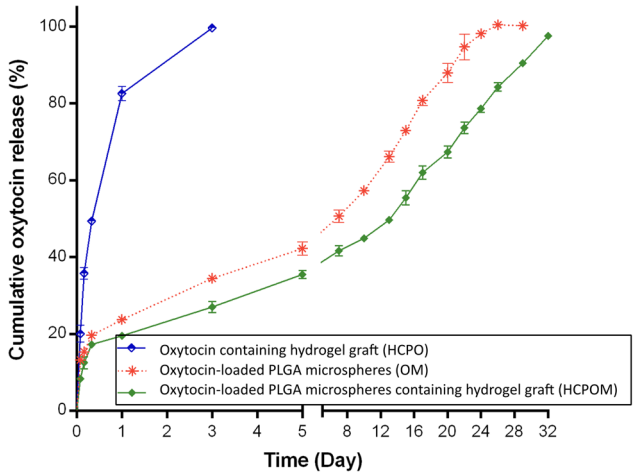

FIGURE 6 In vitro cumulative drug release from oxytocin containing hydrogel graft (HCPO), oxytocin-loaded PLGA microspheres (OM), and oxytocin-loaded PLGA microspheres containing hydrogel graft (HCPOM) (n = 3). PLGA, poly(D, L-lactide-co-glycolide) [Color figure can be viewed at wileyonlinelibrary.com]

other groups. Bone growth deriving from the defect borders was evident in all groups. Complete closure of the defect was possible in none of the groups.

The differences of BMD values were statistically significant at both periods (ANOVA F(1,72) = 8.199; $P = .0055$). After 4 weeks, HCPOM showed the highest mean BMD of 42.21 g/cm^3 (SD, 5.14) with statistically significant differences between control ($P = .0027$) and HCP groups ($P = .0003$). After 8 weeks, HCPOM achieved a mean BMD of 46.94 g/cm^3 (SD, 3.30).

There were no statistically significant changes in BV values in the periods ($P = .72$), however, the differences between the groups were statistically significant (ANOVA F(3,72) = 18.1; $P < .0001$) and HCPOM demonstrated the highest BV of 18.44 mm^3 (SD, 2.58), which the differences between the HCPM and the control were statistically significant ($P = .0044$ and $P < .0001$, respectively). At the end of the 8th week, BV remained almost similar, and a statistically significant difference was observed only between the HCPOM and the control group ($P = .0138$) (Figures 7A and 8A,B).

3.5 | Fluorescence imaging

Orange staining demonstrated the initiation of the bone mineral deposition within the early stages of the healing (10th day). The osteogenic activity was dense at the defect borders, especially in the HCPOM group (orange staining). In the later stages of healing (between the 4th and 8th week), ongoing bone turnover was evident in all groups (orange and green staining). In the control defect, large trabeculae growing from the host bone revealed the typical bone repair process (Figure 7B).

3.6 | Histological observations

Healthy bone formation and osteogenic cell infiltration without any significant inflammation or foreign body reaction were observed. The new bone was evident in all groups deriving from the margins of the defect towards the center at the end of the 8th week.

The graft was penetrated from the defect borders of the native bone and the remnants were remarkable at the edge of the defects in all groups - were mostly seen as a thin layer at the center (Figure 7C).

At the end of the 8th week, complete closure of the defect was not achieved in any of the groups, and new bone islands were visible in some of the HCPOM sections. Phagocytic cell infiltration was dense inside of all of the grafts at both time intervals (Figure 9).

3.7 | Histomorphometric findings

The new bone formation was weak in all groups except the HCPOM. The differences between NB% were statistically significant at both time points. At the 4th week, an average NB of 10% was observed in the HCP, HCPM, and the control groups, whereas HCPOM group revealed 26.45% (SD, 6.65), the difference between the other groups were statistically significant ($P < .0001$). Similarly, the highest NB% of 30.76 (SD, 4.37) in the 8th week was revealed in HCPOM group ($P < .0001$). The change of NB values in between the 4th and the 8th week in the HCPOM group was not statistically significant, -revealing an accelerated bone formation in the HCPOM group at the earlier stages of healing. NB showed a slight increase at the 8th week (13.39% [SD, 5.93], 12.92% [SD, 5.48], and 12.80% [SD:7.63] for the control, HCPM, and HCP groups, respectively) (Figure 8C).

Hydrogel grafts were biodegraded within the 4 weeks in all groups except the HCPM (32.14%; SD, 8.83). The differences of RGs were statistically significant only at the 4th week (ANOVA, F(1,48) = 22.82; $P < .0001$), and the lowest value was observed in HCPOM group (14.36%; SD, 13.01) whereas HCPM yielded the highest value (33.22% [SD, 14.44]; $P = .0046$) (Figure 8D).

4 | DISCUSSION

In this study, a novel thermosensitive hydrogel bone graft combined with oxytocin-loaded PLGA microspheres and the mixture of hydroxyapatite and β-tricalcium phosphate (HCPOM) provided an increased new bone formation and bone mineral density after 4 weeks of healing in 8-mm-diameter rat calvarial defect. The presently selected healing periods (4th and 8th weeks) are of the most frequently employed time points for similar bone-graft experiments in the rat calvaria.[29–31] It should also be emphasized that biological response and regenerative effect of such materials at the early stages of biomaterial healing is of more importance. Long-term biology and bone turnover should be examined by further studies on the basis of recipient areas' requirements.

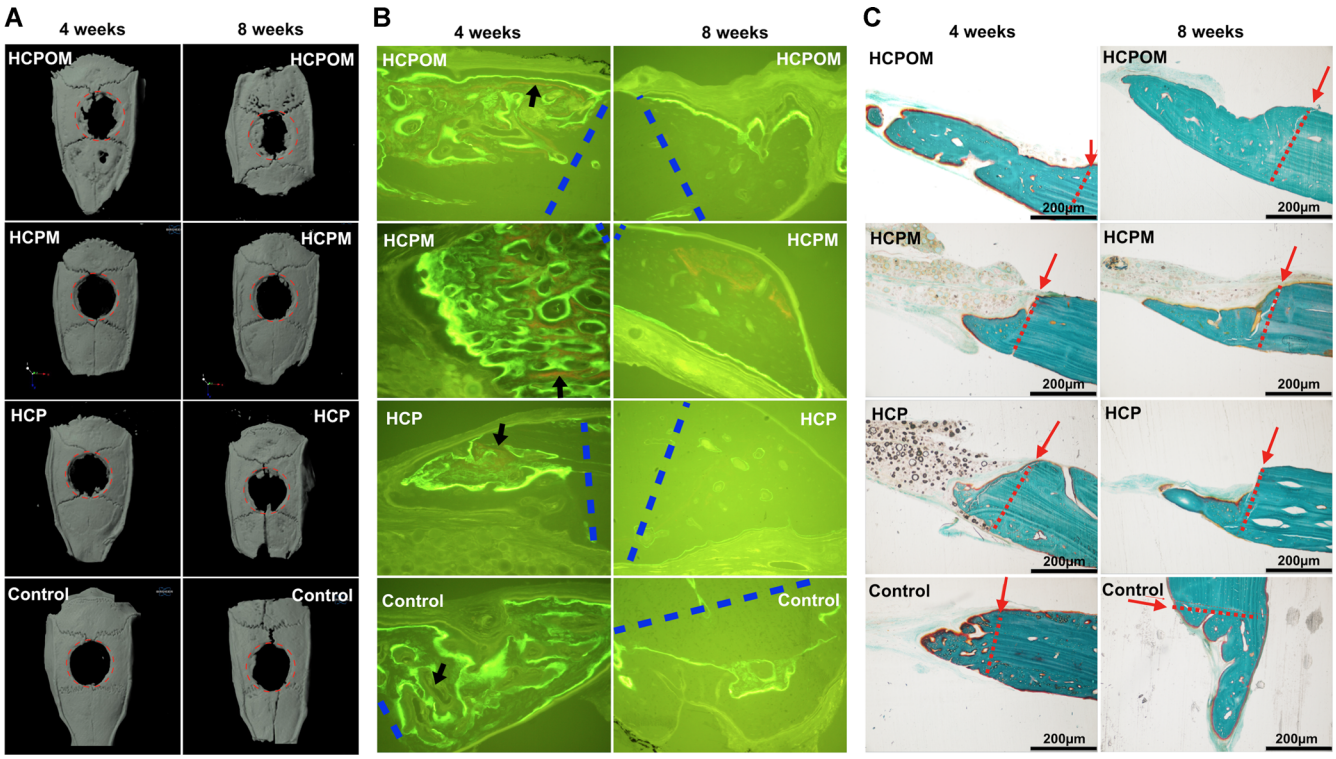

FIGURE 7 A, 3D-reconstructed micro-CT images from the 4th and 8th week of healing. In all groups, bone growth was deriving from the borders of the experimental defect. Complete closure of the defect was possible in none of the groups. Prominent growth of the new bone was observable in the HCPOM group, whereas the healing pattern was resembling the control group in the remaining groups. Intermittent lines represent the original defect border. B, Fluorescence microscopic images from the early- (4th week) and late-term (8th week) healing periods. Alizarin Red (orange staining; injected 10 days after the surgery) and Calcein Green (light green staining; injected 15 days before the sacrification) staining. Blue intermittent lines indicate the defect border. Light green and orange staining layers (arrows) in the HCPOM, HCPM, and HCP groups yielding bone mineral deposition in the early stages of healing. In the later stages of healing, ongoing bone turnover (light green staining) was visible towards the center of the defects. The lack of orange staining the control group yields a slower progression of the new bone growth. Original magnification ×20. C, Histological view of the healing in low magnification (original magnification ×10, Goldner's Masson Trichrome staining). The new bone formation deriving from the edge of the native bone was visible in all sections. A higher amount of new bone formation was evident in the HCPOM group during the 4th week. In the 8th week, graft remnants were scarce in the HCPOM group [Color figure can be viewed at wileyonlinelibrary.com]

Injectability and thermosensitive rheology of the poloxamer at a concentration of 23% facilitated the application and manipulation in the presence of bleeding as well as maintained the structural integrity of the graft components throughout the healing period. On the other hand, the absence of oxytocin hormone in the hydrogel graft formulation (HCP and HCPM groups) resulted in similar NB gain to that of the empty defect.

A similar positive effect of oxytocin hormone on bone regeneration was discerned by Park and coworkers who applied the same amount of oxytocin without a carrier system which was described as "a single administration by simple adsorption to the bone graft" by the authors.[30] Nevertheless, the direct application of this hormone compromises its structural integrity and consequent efficiency. Oxytocin has a very short half-life in serum,[12] and no consensus has yet been established regarding the optimal dosing for local administration in conjunction with bone grafting. The presently employed maximum single dose of 250 μg oxytocin was decided with reference to another study reporting no systemic adverse reactions by systemic administration of a single 1000 μg/kg dose in rats.[32] Sustained-release may also further improve the safety profile of oxytocin in the presented study. Since oxytocin may cause a senile or endocrine-induced osteoporosis by disrupting the osteoblast-osteoclast equilibrium,[33] this dose could seem to be appropriate but should be adjusted according to the individual requirements. For instance, individuals with osteoporotic disorders may benefit the bone regenerative effect with a lower dose, whereas higher doses may alleviate the onset of side effects. Clinical translation of an effective, safe dose warrants further toxicity studies.

A particulate system (PLGA microspheres) was utilized as a carrier to preserve the structural integrity of oxytocin and to provide a long-term drug release in the local cavity. High EE (89.53%) and the sustained-release characteristics of the presented microspheres may have contributed to the higher NB gain in HCPOM group. Without any carrier, in vitro total cumulative release of the 250 μg oxytocin was completed within 3 to 5 days and exhibited a 16.3% of NB formation.[30] A similar effect was obtained with the release of the hydrogel graft containing free oxytocin in the presented study. Free oxytocin in the hydrogel graft showed the fastest release rate, and

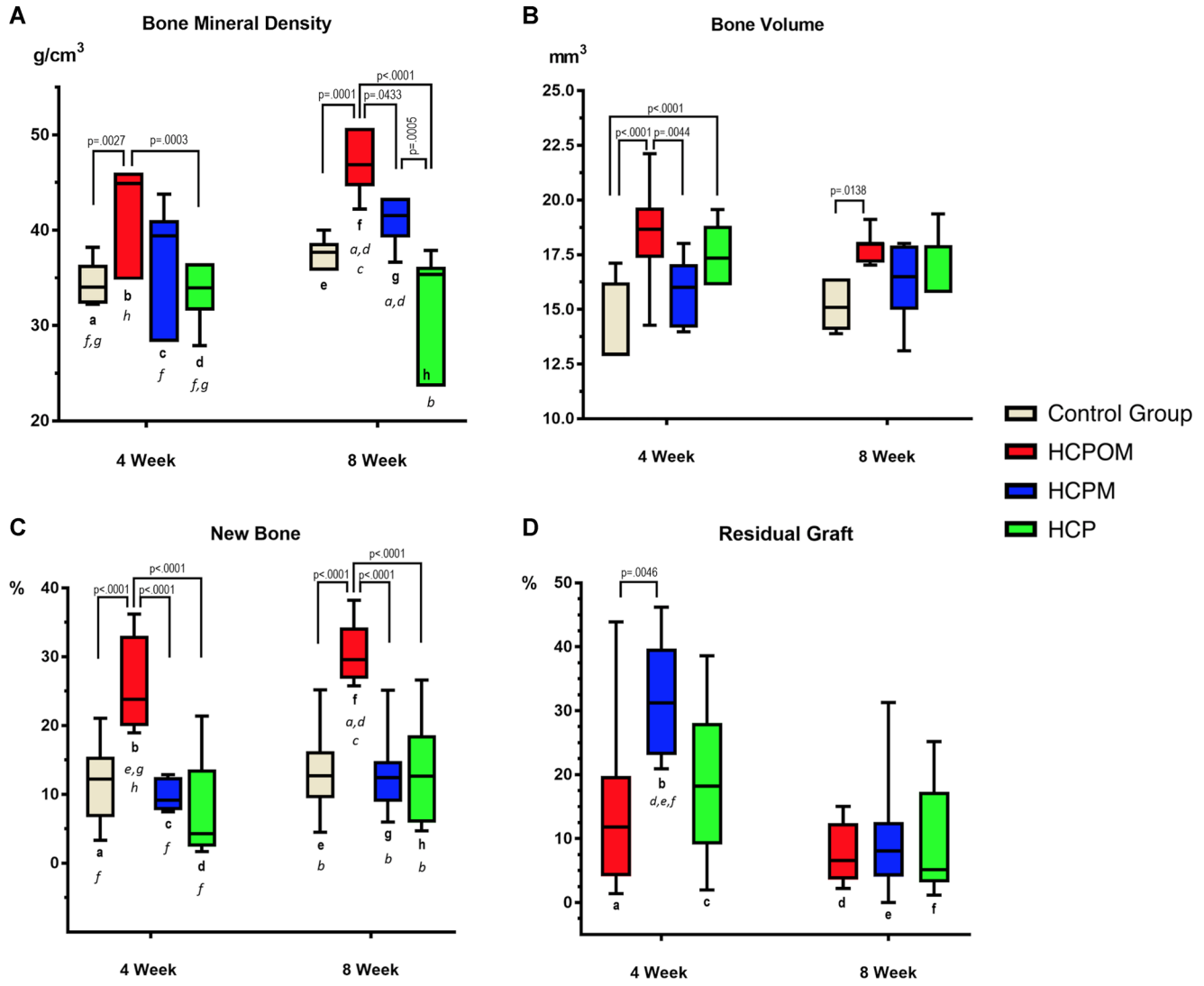

FIGURE 8 A, Box-whisker plot graphics of the bone mineral density (g/cm^3); B, the bone volume (mm^3) measured by micro-CT analysis; C, new bone; and D, residual graft percentage values measured by histomorphometric analysis. Statistically significant differences between the time periods implied by the letters below the bars. RG, residual graft [Color figure can be viewed at wileyonlinelibrary.com]

oxytocin was released entirely within 3 days. Accordingly, this formulation was not tested in vivo. However, the presently described HCPOM extended the release up to 4 weeks and assisted in achieving a NB formation of 30%, approximately.

At a higher level of zeta potential (farther away from 0 mV) results in higher electrostatic repulsion forces between the particles and improves their physical stability by reducing aggregation.[34] In this study, microsphere formulation resulted in a slightly higher positive zeta potential value of 17.4 mV, which is an appropriate value to prevent particle aggregation. PDI results, which expresses dispersion homogeneity in the range between 0 and 1[35] indicated that the particles fabricated in this study were homogeneous.

Thermoreversible systems (such as poloxamer P407) remain liquid below the sol-gel transition temperature and their rheological properties change from liquid-like state to solid-like state above this temperature. The sol-gel transition temperature should be less than body temperature so that it can be easily applied to the local area in a liquid-like state and to improve its remaining time in the solid-like state in the application site at physiological conditions.[36] In this study, the concentration of 23% was chosen due to having the ideal implantable consistency of the hydrogel graft which is easily applicable at lower temperatures and is retained for a long time in the cavity around body temperature.

Similar carrier systems were also proved to provide beneficial effects for bone regeneration with the administration of alternative agents. Yun et al[37] applied a local administration of β-TCP carrier with a parathyroid hormone combination and achieved 15% and 22% of NB formation after 4th and 8th weeks, respectively. Rodríguez-Évora et al[38] used an integrated carrier system containing varying amounts of BMP-2 loaded PLGA microparticles and reported up to 13% and 31% of NB formation after 4th and 8th weeks of healing, respectively. Del Rosario et al[39] tested the combinations of BMP-2, MSC, or PDGF-B with a

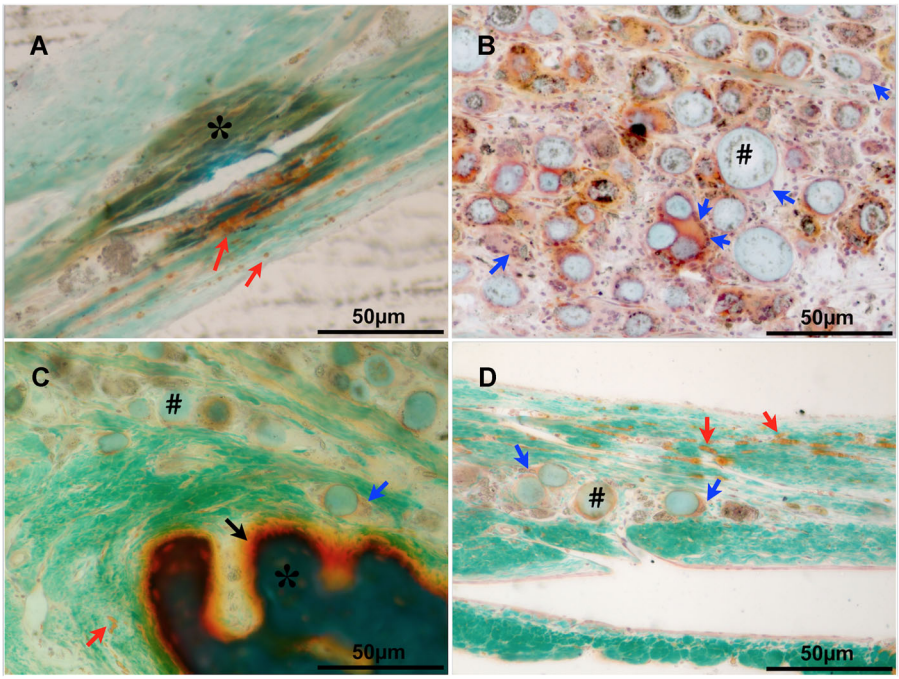

FIGURE 9 Histologic view of the healing in high magnification (original magnification ×40, Goldner's Masson Trichrome staining): A, New bone islands were visible in some of the sections of the HCPOM group at the 8th week. B, Intense phagocytic cell infiltration inside the graft portions of the HCPM group at the 4th week. C, Osteoid tissue synthesis on the host bone and D, osteogenic cell migration towards the center of the defect site was visible in the 4th week of HCPOM group. Blue arrows indicate the phagocytic cell accumulation around the calcium phosphate particles and active phagocytosis of the graft components by phagocytes "#" Calcium phosphate particles. "*" New bone. Red arrows: Osteogenic cells. Blue arrows: phagocytic cells. Black arrows: Osteoid [Color figure can be viewed at wileyonlinelibrary.com]

non-biodegradable macroporous β-TCP scaffold and reached up to 40% of NB in the BMP-2 containing groups. However, this bone gain of the BMP-2 with β-TCP scaffold might be attributed to the employed non-biodegradable character of the scaffold material which could not be compared to the hydrogel used in the presented study. Given these results, it can be concluded that the presently employed oxytocin-loaded grafting system poses a worthy alternative for bone regeneration.

Histomorphometrically measured NB should also be verified by the accumulation of BMD. Hence, the HCPOM group demonstrated the highest amount of BMD in the 4th week, and no other groups achieved such a level of BMD even after 8 weeks. This finding is evident for the apparent positive effect of oxytocin in the earlier stages of bone regeneration. Comparable studies regarding BMD are unfortunately scarce and technically compromised. Without the utilization of a μCT device, 99% of defect coverage was measured by the "digital soft tissue imaging instrument" in the absorbable collagen sponge soaked with recombinant human BMP-2.[31] Yun and coworkers criticized this method due to superposition artifacts that could be sourcing from any "defect covering" material yielded invalid measurements.[37]

Regeneration of a newly formed bone should be accompanied by biodegradation of the biomaterial for allowing the new bone substitution. The high biodegradation rates of the presented hydrogel graft in this study (up to 70% in all groups) could be regarded as satisfactory and evident of favorable degradation dynamics specific to the hydrogels. Oxytocin was, again, a positive inducer for the acceleration of graft biodegradation. The amount of RG was lowest in the HCPOM group (<11%) after 4 weeks of healing. As compared to the reported 50% RG rate of a 12-week healed CAP cement (combined with rhBMP-2-loaded PLGA microspheres),[6] the overall biodegradation performance of the present oxytocin-loaded graft can be regarded as encouraging. The apparent role of oxytocin in this study is also evident from the fact that the groups without oxytocin resemble a healing pattern of an empty control defect which agrees with the reported average bone formation rates of empty rat calvaria defects by Vajgel (9.8 and 12.5% in the 4th and 8th weeks, respectively).[17]

Lastly, it should be underlined that the employed CSD model is rather demanding for bone regeneration and biodegradation since osteogenic cells have to migrate from the border of the large circular defect towards the center. A four- or three-walled defect would sustain an abundance of bone cells and consequently return better results for any of the assessed parameters in the presented study.

Even though the recent animal model and the healing periods have been consigned according to the current literature, it should be noted that a 4 to 8 weeks healing period in an 8-mm-diameter rat calvarial bone may not precisely represent the exact healing outcome in the human jaw bone.[20]

5 | CONCLUSION

Sustained-release of oxytocin hormone loaded into the presented hydrogel graft system provides an increased new bone formation, bone mineral density, and rapid biodegradation within the initial 4 weeks of healing in the critical-sized calvarial bone defects in rats.

ACKNOWLEDGMENTS

This work was supported by the Research Fund of Istanbul University, Project No 50527. This article is an extract of the doctoral thesis of Ayse Sumeyye Akay (supported by the TUBITAK 2211-National Doctorate Scholarship Programme) submitted to the Institute of Health Sciences of Istanbul University in 2017. Authors would like to thank Prof Özgür Özyiğit and Prof Zekeriya Nur from Uludag University for the guidance at the histological examination; Assist Prof Leyla Türker Şener for the assistance at μCT analysis in 3D Medical and Industrial Design Laboratory of Istanbul University (TETLAB); Deniz Morina for the assistance at laboratory studies; Dr Nuriye Ertan Açıkgöz for the statistical counseling; Prof Dr Alper Alkan for the coordination of the non-decalcified histological bone sections.

CONFLICT OF INTERESTS

The authors confirm that there are no known conflicts of interest associated with this publication and there has been no significant financial support for this work that could have influenced its outcome. All authors are full-time academic staff and report no conflict of interest related to any brand, item or entity mentioned in this manuscript.

AUTHOR CONTRIBUTIONS

ASA designed and prepared the study structure conducted the surgeries and experiments collected the results and wrote, revised and approved the final manuscript. VA constructed the study design and the experimental flow supervised the execution of the experiments and data collection analyzed and interpreted the results wrote and approved the revision and the final manuscript. MS and EC played a role in the study design prepared and provided the active components in the experiments interpreted the results and played role in the writing, revision and approval of the manuscript. All authors have read and approved the final article.

ORCID

Volkan Arısan http://orcid.org/0000-0002-0881-7483

REFERENCES

1. Fernandez de Grado G, Keller L, Idoux-Gillet Y, et al. Bone substitutes: a review of their characteristics, clinical use, and perspectives for large bone defects management. *J Tissue Eng.* 2018;9:20417314 18776819.
2. Winkler T, Sass F, Duda G, Schmidt-Bleek K. A review of biomaterials in bone defect healing, remaining shortcomings and future opportunities for bone tissue engineering: the unsolved challenge. *Bone Joint Res.* 2018;7(3):232-243.
3. Arisan V, Özdemir T, Anil A, et al. Injectable calcium phosphate cement as a bone-graft material around peri-implant dehiscence defects: a dog study. *Int J Oral Maxillofac Implants.* 2008;23(6):1053-1062.
4. Li G, Li P, Chen Q, Thu HE, Hussain Z. Current updates on bone grafting biomaterials and recombinant human growth factors implanted biotherapy for spinal fusion: a review of human clinical studies. *Curr Drug Deliv.* 2019;16(2):94-110.
5. Dahlin C, Obrecht M, Dard M, Donos N. Bone tissue modelling and remodelling following guided bone regeneration in combination with biphasic calcium phosphate materials presenting different microporosity. *Clin Oral Implants Res.* 2015;26(7):814-822.
6. Bodde EW, Boerman OC, Russel FG, Mikos AG, Spauwen PH, Jansen JA. The kinetic and biological activity of different loaded rhBMP-2 calcium phosphate cement implants in rats. *J Biomed Mater Res A.* 2008;87(3):780-791.
7. Habraken WJEM, Liao HB, Zhang Z, et al. In vivo degradation of calcium phosphate cement incorporated into biodegradable microspheres. *Acta Biomater.* 2010;6(6):2200-2211.
8. Wozney J, Rosen V, Celeste A, et al. Novel regulators of bone formation: molecular clones and activities. *Science.* 1988;242(4885):1528-1534.
9. Colaianni G, Sun L, Di Benedetto A, et al. Bone marrow oxytocin mediates the anabolic action of estrogen on the skeleton. *J Biol Chem.* 2012;287(34):29159-29167.
10. Colaianni G, Di Benedetto A, Zhu L-L, et al. Regulated production of the pituitary hormone oxytocin from murine and human osteoblasts. *Biochem Biophys Res Commun.* 2011;411(3):512-515.
11. Tamma R, Colaianni G, Zhu L, et al. Oxytocin is an anabolic bone hormone. *Proc Natl Acad Sci USA.* 2009;106(17):7149-7154.
12. Dawood M. Novel approach to oxytocin induction-augmentation of labor. Application of oxytocin physiology during pregnancy. *Adv Exp Med Biol.* 1995;395:585-594.
13. Makadia HK, Siegel SJ. Poly lactic-co-glycolic acid (PLGA) as biodegradable controlled drug delivery carrier. *Polymers.* 2011;3(3):1377-1397.
14. Rice JJ, Martino MM, De Laporte L, Tortelli F, Briquez PS, Hubbell JA. Engineering the regenerative microenvironment with biomaterials. *Adv Healthcare Mater.* 2013;2(1):57-71.
15. Akash MSH, Rehman K. Recent progress in biomedical applications of Pluronic (PF127): pharmaceutical perspectives. *J Controlled Release.* 2015;209:120-138.
16. Torcello-Gómez A, Wulff-Pérez M, Gálvez-Ruiz MJ, Martín-Rodríguez A, Cabrerizo-Vílchez M, Maldonado-Valderrama J. Block copolymers at interfaces: interactions with physiological media. *Adv Colloid Interface Sci.* 2014;206:414-427.
17. Vajgel A, Mardas N, Farias BC, Petrie A, Cimões R, Donos N. A systematic review on the critical size defect model. *Clin Oral Implants Res.* 2014;25(8):879-893.
18. Lee DJ, Padilla R, Zhang H, Hu WS, Ko CC. Biological assessment of a calcium silicate incorporated hydroxyapatite-gelatin nanocomposite: a comparison to decellularized bone matrix. *BioMed Res Int.* 2014;2014:12.
19. Magaye RR, Yue X, Zou B, et al. Acute toxicity of nickel nanoparticles in rats after intravenous injection. *Int J Nanomedicine.* 2014;9:1393-1402.
20. Sun TC, Mori S, Roper J, Brown C, Hooser T, Burr DB. Do different fluorochrome labels give equivalent histomorphometric information? *Bone.* 1992;13(6):443-446.
21. Donovan J, Brown P. Parenteral injections. *Curr Protoc Neurosci.* 2006; 73(1):1-6.
22. Hahn M, Vogel M, Delling G. Undecalcified preparation of bone tissue: report of technical experience and development of new methods. *Virchows Archiv A.* 1991;418(1):1-7.
23. Yang R, Davies CM, Archer CW, Richards RG. Immunohistochemistry of matrix markers in Technovit 9100 new-embedded undecalcified bone sections. *Eur Cell Mater.* 2003;6:57-71.
24. Rentsch C, Schneiders W, Manthey S, Rentsch B, Rammelt S. Comprehensive histological evaluation of bone implants. *Biomatter.* 2014; 4(1):e27993.

25. Zhao J, Hu J, Wang S, et al. Combination of β-TCP and BMP-2 gene-modified bMSCs to heal critical size mandibular defects in rats. *Oral Dis*. 2010;16(1):46-54.
26. Requicha JF, Moura T, Leonor IB, et al. Evaluation of a starch-based double layer scaffold for bone regeneration in a rat model. *J Orthop Res*. 2014;32(7):904-909.
27. Chanchareonsook N, Junker R, Jongpaiboonkit L, Jansen JA. Tissue-engineered mandibular bone reconstruction for continuity defects: a systematic approach to the literature. *Tissue Eng Part B Rev*. 2013;20(2):147-162.
28. Bongio M, van den Beucken JJ, Leeuwenburgh SC, Jansen JA. Preclinical evaluation of injectable bone substitute materials. *J Tissue Eng Regener Med*. 2015;9(3):191-209.
29. Histing T, Garcia P, Holstein JH, et al. Small animal bone healing models: standards, tips, and pitfalls results of a consensus meeting. *Bone*. 2011;49(4):591-599.
30. Park JW, Kim JM, Lee HJ, Jeong SH, Suh JY, Hanawa T. Bone healing with oxytocin-loaded microporous β-TCP bone substitute in ectopic bone formation model and critical-sized osseous defect of rat. *J Clin Periodontol*. 2014;41(2):181-190.
31. Stancoven BW, Lee J, Dixon DR, et al. Effect of bone morphogenetic protein-2, demineralized bone matrix and systemic parathyroid hormone (1-34) on local bone formation in a rat calvaria critical-size defect model. *J Periodont Res*. 2013;48(2):243-251.
32. Petersson M, Wiberg U, Lundeberg T, Uvnäs-Moberg K. Oxytocin decreases carrageenan induced inflammation in rats. *Peptides*. 2001;22(9):1479-1484.
33. Prakash D, Behari J, eds. Synergistic role of hydroxyapatite nanoparticles and pulsed electromagnetic field therapy to prevent bone loss in rats following exposed to simulated microgravity. International Conference on Recent Advances in Microwave Theory and Applications. IEEE; 2008.
34. Cevher E, Salomon SK, Makrakis A, Li XW, Brocchini S, Alpar HO. Development of chitosan–pullulan composite nanoparticles for nasal delivery of vaccines: optimisation and cellular studies. *J Microencapsul*. 2015;32(8):755-768.
35. Du J, Zhang S, Sun R, Zhang LF, Xiong CD, Peng YX. Novel polyelectrolyte carboxymethyl konjac glucomannan—chitosan nanoparticles for drug delivery. II. Release of albumin in vitro. *J Biomed Mater Res B Appl Biomater* 2005;72(2):299-304.
36. Galgatte UC, Chaudhari PD. Preformulation study of poloxamer 407 gels: effect of additives. *Int J Pharm Pharm Sci*. 2014;6(1):130-133.
37. Yun JI, Wikesjö UM, Borke JL, et al. Effect of systemic parathyroid hormone (1-34) and a β-tricalcium phosphate biomaterial on local bone formation in a critical-size rat calvarial defect model. *J Clin Periodontol*. 2010;37(5):419-426.
38. Rodríguez-Évora M, Delgado A, Reyes R, et al. Osteogenic effect of local, long versus short term BMP-2 delivery from a novel SPU-PLGA-bTCP concentric system in a critical size defect in rats. *Eur J Pharm Sci*. 2013;49:873-884.
39. Del Rosario C, Rodríguez-Évora M, Reyes R, Delgado A, Évora C. BMP-2, PDGF-BB, and bone marrow mesenchymal cells in a macroporous β-TCP scaffold for critical-size bone defect repair in rats. *Biomed Mater*. 2015;10(4):045008.

How to cite this article: Akay AS, Arısan V, Cevher E, Sessevmez M, Cam B. Oxytocin-loaded sustained-release hydrogel graft provides accelerated bone formation: An experimental rat study. *J Orthop Res*. 2020;38:1676–1687. https://doi.org/10.1002/jor.24607